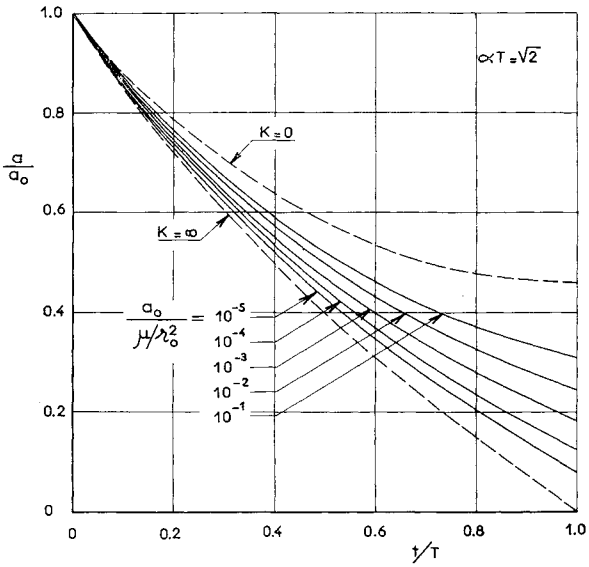

Fig. 1 Optimum thrust acceleration programs for escape from satellite orbit

where

$$K = \frac{1}{\alpha}\frac{(dU/ds)_T}{V_T} \qquad [11]$$

For the case where V_T is specified and s_T is arbitrary, $a_T = 0$ (1) and, as indicated by Eqs. [9] and [11], $K = 0$; with s_T specified and V_T arbitrary, on the other hand, $a_T = 0$ (1) and $K = \infty$. For the problem of earth-escape, representative values of K can be obtained by assuming that, as a first approximation, a is constant and equal to a_0 along the entire trajectory. Under this assumption the low thrust rocket trajectory data of Ref. 2 can be used directly, giving $\phi_T = 39°$ at the instant when the vehicle velocity is equal to the local parabolic velocity. At burnout, therefore,

$$(dU/ds)_T \cong -(\mu/r_T^2)\sin 39° \qquad [12]$$

whereas the burnout velocity is given by

$$V_T = (2\mu/r_T)^{1/2} \qquad [13]$$

The initial tangential component of gravitational force per unit mass is $2a_0$, whereas at burnout this component is approximately a_0 (2). The range Δs is approximately $V_0\,T/2$, and V_0 is simply $(\varphi/r_0)^{1/2}$. From the definition of α, therefore,

$$\alpha^2 \cong \frac{a_0}{\Delta s} \cong \frac{2a_0}{(\mu/r_0)^{1/2}T} \qquad [14]$$

Finally, from Ref. 2

$$T \cong V_0/a_0 \cong (1/a_0)(\mu/r_0)^{1/2} \qquad [15]$$

and

$$\frac{r_0}{r_T} \cong \left[\frac{a_0}{(\mu/r_0^2)}\right]^{1/2} \qquad [16]$$

The combination of Eqs. [11–16] results in

$$K \cong -\frac{0.31}{\left(\dfrac{a_0}{\mu/r_0^2}\right)^{1/4}} \qquad [17]$$

where the quantity in parentheses in the denominator of the right-hand side represents the ratio of thrust to weight in the initial satellite orbit. The value of αT is obtained by combining Eqs. [14] and [15], giving $\alpha T = (2)^{1/2}$ regardless of the initial thrust-to-weight ratio.[3]

Eq. [10] has been plotted in Fig. 1 for $\alpha T = (2)^{1/2}$ and for values of $a_0 r_0^2/\mu$ varying from 10^{-5} to 10^{-1}. The corresponding values of K were obtained from Eq. [17]. Also shown in Fig. 1 are curves of $a(t)$ for $K = 0$ and for $K = \infty$. It can be seen that, with initial thrust-to-weight ratios of 10^{-5} and 10^{-4}, thrust programs for escape with minimum propellant utilization approach the optimum thrust program for specified range and arbitrary final velocity ($K = \infty$). With larger initial thrust-to-weight ratios, however, optimum thrust programs for escape tend toward the optimum curve for specified final velocity and arbitrary range ($K = 0$). Regardless of the initial thrust-to-weight ratio, the departure of the optimum earth-escape thrust program from that of constant thrust per unit mass is considerable.

References

1 Faulders, C. R., "Optimum thrust programming of electrically powered rocket vehicles in a gravitational field," ARS J. **30**, 954–960 (1960).
2 Perkins, F. M., "Flight mechanics of low thrust space craft," *Vistas in Astronautics* (Pergamon Press Inc., New York, 1959), Vol. II; J. Aerospace Sci. **26**, 291–297 (1959).

[3] This value of αT represents an improvement over the values reported in Table 3 of Ref. 1.

Electrical Discharge Across a Supersonic Jet of Plasma in Transverse Magnetic Field[1]

STERGE T. DEMETRIADES[2] AND PETER D. LENN[3]
Northrop Corporation, Hawthorne, Calif.

Observations have been made of the discharge between two electrodes placed across a supersonic stream of ionized gas. A magnetic field transverse to both the flow direction and the electrode axes was applied. In this note, visual observations of the behavior of the discharge with and without magnetic fields will be described, and qualitative explanations of the observed phenomena will be proposed.

THE experiments described were performed with water-cooled copper electrodes in contact with the cooler outer sheath of a free jet of argon plasma produced by a commercial arcjet (Plasmadyne M-4). Argon gas at a flow rate of 1.36×10^{-3} kg/sec was heated to an average stagnation enthalpy of the order of 8×10^6 j/kg. The plasma entered the region between the electrodes at a velocity of approximately 3×10^4 m/sec and a Mach number of approximately 2.5. The electrode cross-sectional area was 6.45×10^{-4} m^2, and the electrode gap (i.e., the separation between the two electrode surfaces) was 3.8×10^{-2} m. Further details of the apparatus are given elsewhere (1–3).[4]

The contact of the electrodes with the plasma stream at the operating pressures of from 2 to 4 mm Hg generated weak, oblique shock patterns that were faintly but distinctly visible

Received by ARS September 17, 1962.
[1] This work was supported in part by the U. S. Air Force through the Propulsion Division, Directorate of Engineering Sciences, Office of Aerospace Research, Air Force Office of Scientific Research, under Contract AF 49(638)-1160.
[2] Head, Plasma Laboratories. Senior Member ARS.
[3] Member of Research Staff, Plasma Laboratories. Member ARS.
[4] Numbers in parentheses indicate References at end of paper.

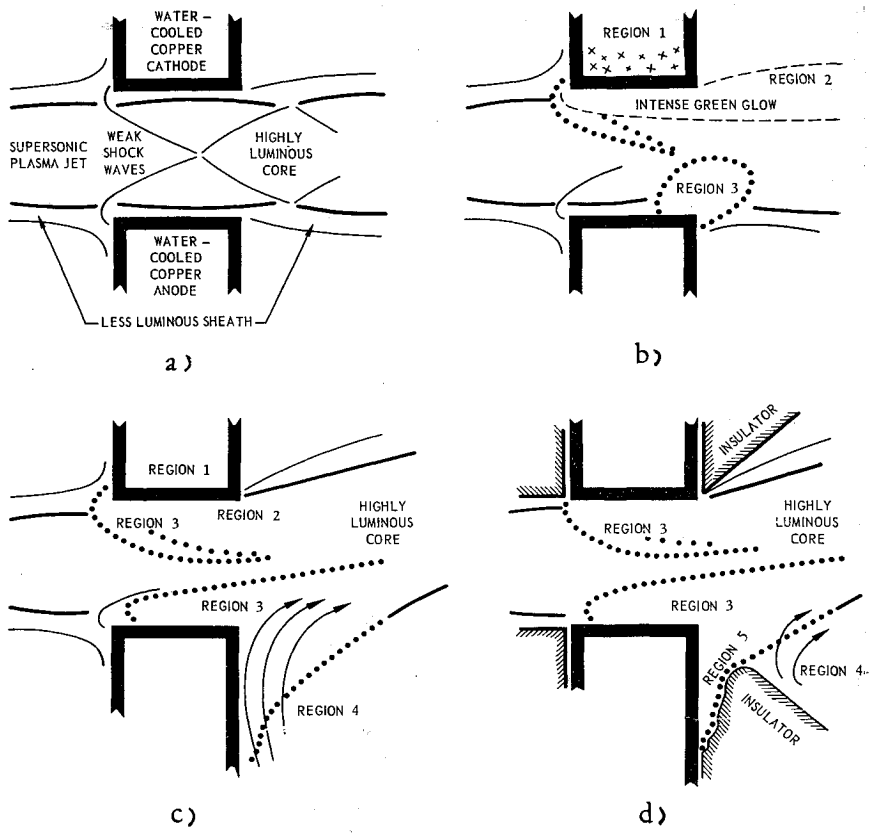

Fig. 1 Schematic of main features of continuous stable discharge across a supersonic jet of plasma in a transverse magnetic field. The magnetic field is perpendicular to the plane of the figure and directed towards the reader. a) Free jet of plasma flowing between electrodes. b) Same with electric current on, no magnetic field; region 1, large number of random simultaneous sparks on copper cathode surface; region 2, intense green glow; region 3, intense white glow. c) Same as Fig. 1b but with magnetic field on (B > 2000 gauss); region 1, sparks disappear (B > 500 gauss); region 2, green glow disappears (B > 500 gauss); region 3, intense white glow spreads upstream on anode surface and down trailing side of anode; region 4, flow pattern may feed some ambient gas into magnetic field region. d) Same as Fig. 1c but with insulator surrounding electrodes; region 3 essentially unaltered; region 4, insulator, when intact, prevents feeding of discharge by ambient gas; but, region 5, insulator burns

in the luminous jet. The electrode gap was centered between the 3-in.-diam poles of an electromagnet that provided a field transverse to the flow direction and to the electric field supplied by the electrodes. The pole piece of one of the magnet coils was removed to provide an observation port into the accelerator. This produced an asymmetrical magnetic field that varied in a typical situation from 2300 gauss at the side of the channel near the remaining pole piece to 1400 gauss at the side near the coil from which the pole had been removed. The applied electrical potential varied from approximately 25 v at an applied magnetic field of $B = 0$ gauss to approximately 100 v at $B \approx 2000$ gauss while the current through the gas was maintained constant at several hundred amperes (1–3). All observations and performance data were qualitatively similar to those obtained with a symmetrical field of strength equal to that found along the centerline of the asymmetrical field (2). No noticeable horizontal deflection of the exhaust jet from the centerline of the channel was produced by the asymmetrical magnetic field.

The phenomena observed are pictured schematically in Fig. 1. Fig. 1a shows the stream of plasma from the arcjet passing through the accelerator section when neither electric nor magnetic fields are applied. The central core of the flow was highly luminous. Its color varied from white at the center to pink farther out and finally to deep purple in the outermost visible sheath. Application of a magnetic field alone, transverse to the flow, decelerated the plasma and generated currents that flowed either through an external load resistance connected to the electrodes or through closed loops within the plasma itself when the electrodes were not connected externally. The deceleration of the supersonic stream by the application of only the magnetic field caused a sizable contraction in the cross-sectional area of the supersonic jet.

Passing a current of several hundred amperes from an external source between the electrodes when no magnetic field was applied produced the situation sketched in Fig. 1b. The prominent features were as follows: 1) A multitude of simultaneous, random sparks appeared on the surface of the cathode (region 1 in Fig. 1b). 2) A bright green luminosity was observed over the surface of the cathode and downstream of the cathode, making the upper part of the exhaust plume green (region 2 in Fig. 1b) while the lower part was pink-violet. This coloration persisted until the exhaust cooled off several feet downstream of the electrode gap. The green luminosity was similar to that of a copper flame test. The thickness of region 2 over the cathode is exaggerated in Fig. 1b. 3) A very intense, white luminosity emanated from the plasma at the trailing edge of the anode (region 3 in Fig. 1b), and a narrow region of almost similar intensity extended in an arc from the leading edge of the cathode until it almost reached the luminous region at the trailing edge of the anode.

When the applied magnetic field was increased from zero while the electric current was flowing, the following events occurred: 1) As the magnetic field strength increased, the random simultaneous sparks on the cathode surface became less frequent and less distinct and disappeared completely at approximately 500 gauss (0.05 weber/m^2). 2) The green luminosity emanating from the cathode also decreased and completely disappeared at magnetic field strengths above about 500 gauss. 3) As the magnetic field increased, the exhaust plume deflected upward by an amount that increased with field strength. The deflection at 500 gauss and an accelerator current of 400 amp was less than 5°. 4) The intense white glow at the trailing edge of the anode spread upstream on the top surface and down the trailing side of the anode (region 3 in Fig. 1c). At the same time, the region of intense luminosity which extended from the leading edge of the cathode became slightly thicker when the magnetic field was increased but was otherwise unchanged. 5) The flow pattern downstream of the anode (region 4 in Fig. 1c) seemed to feed some ambient gas into the discharge within the region of influence of the magnetic field.

The situation shown schematically in Fig. 1d is found to occur when the flow is confined and the downstream sides of the electrodes are covered with insulating materials (2). The insulator downstream of the anode, when intact, prevents feeding of the discharge by ambient gas. However, it spalls

from thermal stress and/or ablates (region 5 in Fig. 1d). The discharge is otherwise essentially the same as in the unconfined channel.

The random sparking that occurs at the cathode surface in the absence of the applied magnetic field is most likely due to sputtering associated with the bombardment of the cathode by energetic ions. Sputtering erodes the copper cathode and would account for the green coloration, characteristic of copper, which is observed in the cathode wake. The applied magnetic field diminishes the frequency and intensity of the random sparking on the cathode and the luminosity of the copper-green wake that trails from the cathode and causes both effects to disappear at fields of more than 500 gauss. Erosion of the cathode also effectively stops at 500 gauss. A possible reason for this is that the number of energetic ions that strike a given spot of the cathode surface is reduced with increasing magnetic field.

Since the maximum energy of the ions in these experiments cannot be much in excess of 25 to 100 ev, the random multiple sparks probably do not arise from the collision of single, very high energy ions with the cathode surface but are probably the result of a local collapse of positive space charge column(s) on the cathode. Each collapsing column consists of many ions of moderate energy (from a fraction of an electron volt to several electron volts). The combined energy of these ions hitting the same spot in quick succession drives a thermal spike into the cathode surface at the point of impact (the base of the column). Many of these thermal spikes possess sufficient energy to cause local sputtering of the copper cathode, and the multiple jets are visible as multiple sparks distributed at random over the cathode surface. The sputtered copper causes the green luminosity of the cathode wake. Then one of the possible mechanisms causing the suppression and eventual disappearance of the sparks and the green luminosity with increasing B is the bending of the trajectories of the moderate energy ions or ion clusters by the applied magnetic field. In that case, the ions at the top of the collapsing column will strike a different spot on the cathode from the ions at the bottom of the column and will effectively smear out the energy input to the surface so that the thermal spike is attenuated. For example, if a 10^{-3}-m-long column of monoenergetic ions (of the order of 10^4 ions under the conditions of the experiment) with a velocity of 3×10^3 m/sec (corresponding to 2 ev or the drift velocity, which results when an electric field of 150 v/m and a transverse magnetic field of 0.05 weber/m^2 are acting on the ions) collapses in the presence of a magnetic field of 0.05 weber/m^2, it will spread out on the surface of the cathode over a length of the order of $\Delta x \approx (10^{-3})^2/2r_c$ m, where r_c is the cyclotron radius given by $r_c = 4.18 \times 10^{-7}\,(U/B) = 2.5 \times 10^{-2}$ m, i.e., over $\Delta x = 2 \times 10^{-5}$ m, or roughly over 10^4 atoms of copper. Note that under these conditions the ions that are more than 5×10^{-2} m away from the cathode can never even reach it without collisions. Collisions, however, would tend to reduce their energy amd make their impacts even less effective. This computation is not meant to be quantitative; nevertheless, it indicates a possible mechanism that could account for the disappearance of the random sparks and the copper-green wake. Note also that, if the sparks were the result of impacts of single high energy ions on the cathode surface, the slight deflection of their trajectories by the magnetic field would have no effect on the frequency and intensity of the sparks.

Other possible explanations for these phenomena are that 1) the magnetic field causes the cathode spot(s) to move rapidly on the cathode surface, thereby spreading out the energy input and broadening the thermal spikes, and/or 2) the magnetic field causes a decrease of the energy of the incident ions.

As the magnetic field strength increases, the luminous region that is initially concentrated at the trailing edge of the anode (region 3, Fig. 1b) spreads upstream on the top surface and down the trailing side of the anode. The spreading of the highly luminous sheath over the surface of the anode is associated with the increased impedance of the plasma in the direction of the applied electric field (perpendicular to the applied magnetic field) which increases the cross-sectional area of the discharge and the applied voltage (for constant current). The increased applied voltage also contributes to the spreading of the discharge upstream on the anode surface, i.e., toward the accelerator inlet where the back emf UB is small. This increase of the impedance across the electrode gap enhances the tendency of the discharge to fringe outside the gap and outside the region of influence of the applied magnetic field.

The vertical deflection of the exhaust plume mentioned previously which increases with increasing magnetic field is produced by the interaction of the applied magnetic field with the axial component of the electric current. The axial component of the current, i.e., the current perpendicular to both the applied magnetic field and the applied electric field, is a Hall current that may be interpreted in terms of the tensor conductivity of a plasma in the presence of a magnetic field. The vertical deflection of the jet can be avoided by moving the anode upstream of the cathode so as to provide an axial component of electric field which suppresses the axial current.

The observations reported here were made visually and photographically and therefore are descriptions of the intensity of visible light radiated from various points in the plasma flow. From the nature of the patterns described, it seems reasonable to assume that the regions of high luminosity correspond to those of high current density and the associated high rate of ohmic heating. Experimental investigations to determine the current distribution more precisely through the use of spectroscopic, microwave, and induction-coil probing techniques are currently in progress at the Northrop Plasma Laboratories.

References

1 Demetriades, S. T., "Experimental magnetogasdynamic engine for argon, nitrogen and air," ASRL-TM-60-23, Norair Div., Northrop Corp. (November 1960); also *Engineering Aspects of Magnetohydrodynamics: Proceedings of Second Symposium on Engineering Aspects of MHD* (Columbia University Press, New York, 1962), pp. 19–44.

2 Demetriades, S. T., "Experiments with a high specific impulse crossed-field accelerator," NSL-62-130, Northrop Space Labs., Northrop Corp. (July 1962); presented at Third Symposium on Engineering Aspects of Magnetohydrodynamics, University of Rochester, March 28–30, 1962 (Proceedings to be published).

3 Demetriades, S. T., Hamilton, G. L., Ziemer, R. W., and Lenn, P. D., "Three-fluid non-equilibrium plasma accelerators, Part 1," ARS Preprint 2375-62 (March 1962).

A Class of Linear Magnetohydrodynamic Flows

M. R. El-Saden*

North Carolina State College, Raleigh, N. C.

Introduction

THE continuity and momentum equations for the steady laminar flow of a conducting fluid of constant properties, that is, constant fluid density ρ, viscosity μ, and electrical conductivity σ, are

$$\nabla \cdot V = 0 \tag{1}$$

$$\rho(V \cdot \nabla)V + \nabla P = J \times B + \mu \nabla^2 V \tag{2}$$

where V is the velocity vector, with components u, v, and w in

Received by ARS October 31, 1962.

* Associate Professor of Mechanical Engineering. Member, ARS.